Surface Thermolytic Behavior of Nickel Amidinate and Its Implication on the Atomic Layer Deposition of Nickel Compounds

Ran Zhao,[1] Shuang Xiao,[2,3] Shihe Yang,[2,3] and Xinwei Wang[1,*]

1. School of Advanced Materials, Shenzhen Graduate School, Peking University, Shenzhen 518055, China

2. Guangdong Key Lab of Nano-Micro Material Research, School of Chemical Biology and Biotechnology, Shenzhen Graduate School, Peking University, Shenzhen 518055, China

3. Department of Chemistry, The Hong Kong University of Science and Technology, Clear Water Bay, Kowloon, Hong Kong

*E-mail: wangxw@pkusz.edu.cn

Table S1. Fitting results of the Ni 2p$_{3/2}$ XPS spectra shown in Figure 1. (Bold font denotes the fixed parameters during fitting.)
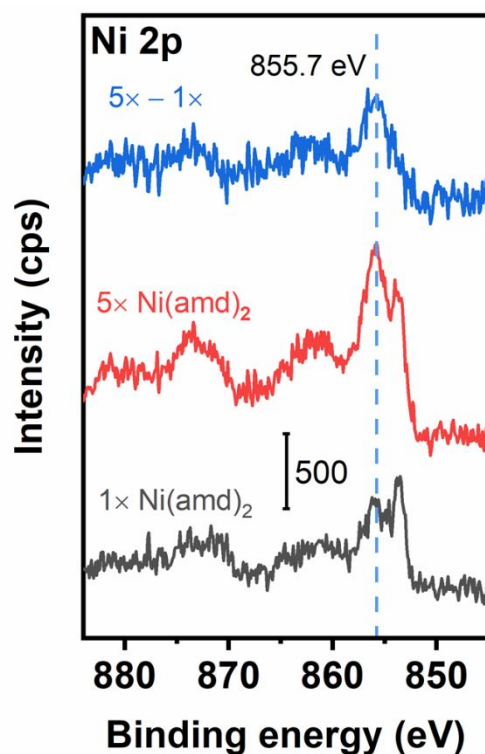
Temperature (°C)	Ni−O									Ni-metallic								
	Main peak			Satellite component 1			Satellite component 2			Main peak			Satellite component 1			Satellite component 2		
	BE (eV)	Width (eV)	Area (cps eV)	BE (eV)	Width (eV)	Area (cps eV)	BE (eV)	Width (eV)	Area (cps eV)	BE (eV)	Width (eV)	Area (cps eV)	BE (eV)	Width (eV)	Area (cps eV)	BE (eV)	Width (eV)	Area (cps eV)
SiO$_x$/Si	-	-	-	-	-	-	-	-	-	-	-	-	-	-	-	-	-	-
25	856.5	3.1	17744.7	861.4	4.0	11103.5	865.1	4.0	5931.3	-	-	-	-	-	-	-	-	-
100	856.5	3.1	19345.0	861.4	4.0	12150.1	865.1	4.0	6113.0	-	-	-	-	-	-	-	-	-
150	856.7	**3.1**	20053.8	**861.6**	**4.0**	12633.9	**865.3**	**4.0**	6617.7	**853.7**	**1.9**	650.7	**855.7**	**3.5**	246.6	**859.5**	**3.5**	191.8
200	856.8	**3.1**	19747.1	**861.7**	**4.0**	12440.6	**865.4**	**4.0**	6516.5	**853.7**	**1.9**	1321.2	**855.7**	**3.5**	458.9	**859.5**	**3.5**	389.4
250	856.9	**3.1**	8762.1	**861.8**	**4.0**	5519.9	**865.5**	**4.0**	2891.5	853.7	**1.9**	9348.4	**855.7**	**3.5**	3084.7	**859.5**	**3.5**	2617.3
300	857.0	**3.1**	3908.4	**861.9**	**4.0**	2462.3	**865.6**	**4.0**	1289.9	853.7	**1.9**	12463.8	**855.7**	**3.5**	4112.9	**859.5**	**3.5**	3489.9
350	857.0	**3.1**	2079.1	**861.9**	**4.0**	1309.9	**865.6**	**4.0**	686.2	853.7	1.9	14139.3	**855.7**	**3.5**	4666.0	**859.5**	**3.5**	3959.0
400	857.1	**3.1**	1530.9	**862.0**	**4.0**	964.5	**865.7**	**4.0**	505.2	853.7	1.9	14157.3	**855.7**	**3.5**	4671.9	**859.5**	**3.5**	3964.0

Table S2. Fitting results of the O 1s XP spectra shown in Figure 2. (Bold font denotes the fixed parameters during fitting.)

| Temperature (°C)	O 1s signal					
	SiO_x			Ni−O		
	BE (eV)	Width (eV)	Area (cps eV)	BE (eV)	Width (eV)	Area (cps eV)
SiO_x/Si	532.8	1.5	56466.8	-	-	-
25	532.8	**1.5**	44862.9	530.9	**1.5**	1742.4
100	532.8	**1.5**	45586.2	**530.9**	1.5	1836.4
150	532.8	**1.5**	48351.5	**530.9**	1.5	1758.5
200	532.8	**1.5**	50423.1	**530.9**	1.5	1524.1
250	532.8	**1.5**	52947.8	**530.9**	1.5	1105.1
300	532.8	**1.5**	53355.4	**530.9**	1.5	1183.6
350	532.8	**1.5**	53802.4	**530.9**	1.5	897.6
400	532.8	**1.5**	53831.8	**530.9**	1.5	860.9

Table S3. Fitting results of the N 1s and C 1s XP spectra shown in Figure 3. (Bold font denotes the fixed parameters during fitting.)

Temperature (°C)	N 1s signal						C 1s signal									Additional carbon		
	N in Ni−amd			N in −OH···Hamd			Carbon in amd											
							Alkyl C			Amido C			Amidine C					
	BE (eV)	Width (eV)	Area (cps eV)	BE (eV)	Width (eV)	Area (cps eV)	BE (eV)	Width (eV)	Area (cps eV)	BE (eV)	Width (eV)	Area (cps eV)	BE (eV)	Width (eV)	Area (cps eV)	BE (eV)	Width (eV)	Area (cps eV)
SiO_x/Si	-	-	-	-	-	-	-	-	-	-	-	-	-	-	-	-	-	-
25	399.0	2.0	5216.3	400.9	**2.0**	826.8	285.5	1.7	15004.8	286.7	**1.7**	**4291.3**	287.5	**1.7**	**2145.6**	-	-	-
100	399.2	**2.0**	5457.2	**400.9**	2.0	817.4	285.6	1.7	14467.5	**286.8**	1.7	**4137.4**	**287.6**	1.7	**2069.0**	-	-	-
150	399.2	**2.0**	4839.7	**400.9**	2.0	540.6	285.5	1.7	10919.1	**286.7**	1.7	**3122.8**	**287.5**	1.7	**1561.4**	-	-	-
200	399.3	**2.0**	4104.5	**400.9**	2.0	90.3	285.5	1.7	8191.9	**286.7**	1.7	**2342.9**	**287.5**	1.7	**1171.4**	-	-	-
250	399.2	**2.0**	1256.1	**400.9**	2.0	62.4	**285.5**	1.7	2552.2	**286.7**	1.7	**729.9**	**287.5**	1.7	**364.9**	285.1	**1.7**	1408.4
300	399.2	**2.0**	407.5	**400.9**	2.0	43.5	**285.5**	1.7	1008.4	**286.7**	1.7	**288.4**	**287.5**	1.7	**144.2**	285.1	1.7	2415.9
350	-	-	-	-	-	-	-	-	-	-	-	-	-	-	-	285.0	**1.7**	3208.0
400	-	-	-	-	-	-	-	-	-	-	-	-	-	-	-	284.9	**1.7**	2843.0

Figure S1. XPS Ni 2p spectra for the Ni(amd)$_2$ dosed directly on HF-cleaned Si at room temperature. A regular Ni(amd)$_2$ dose (1×) and a 5 times larger dose (5×) were used. The top trace shows the difference of the two spectra below. Since the Si surface inevitably contained some active dangling groups, the Ni(amd)$_2$ molecules would first chemically react with these groups (chemisorption). But when excessive Ni(amd)$_2$ vapor was provided, molecular Ni(amd)$_2$ would eventually build up on the top (physisorption) at room temperature (Ni(amd)$_2$ is a solid at room temperature). Accordingly, the 5×–1× differential spectrum (blue color) should represent the spectrum of the physisorbed Ni(amd)$_2$, and therefore the BE of Ni 2p$_{3/2}$ for molecular Ni(amd)$_2$ was found at 855.7 eV.
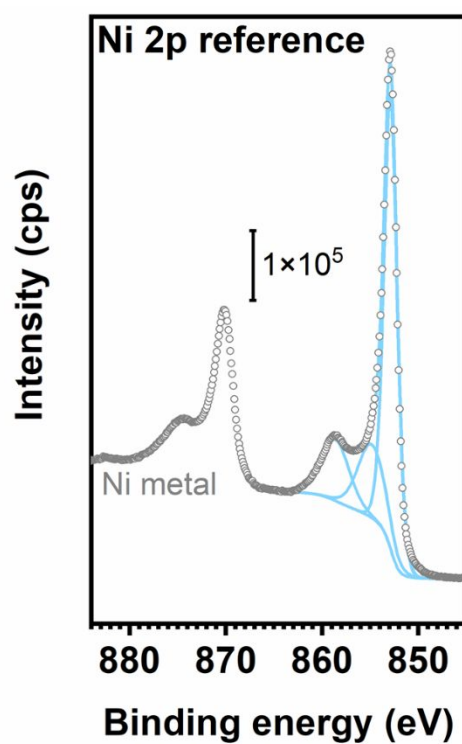
Figure S2. XPS Ni 2p spectrum for bulk Ni metal. The Ni $2p_{3/2}$ peak was fitted by using three peak components, of which one major component at 852.9 eV was used to account for the main peak and two minor components at 854.9 eV and 858.6 eV were together used to account for the satellite band.
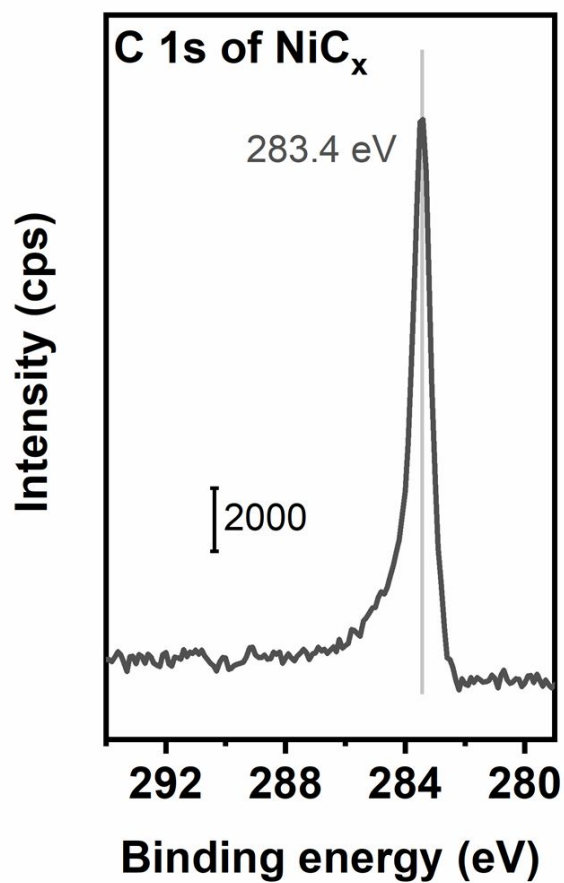
Figure S3. XPS C 1s spectrum for NiC_x, and the BE of the C 1s peak is at 283.4 eV.

The NiC_x sample was prepared by ALD following the literature (*ACS Appl. Mater. Interfaces*, **2018**, 10, 8384−8390).

Table S4. Surface sensitivity factors for quantitative XPS analysis (Figure 5).

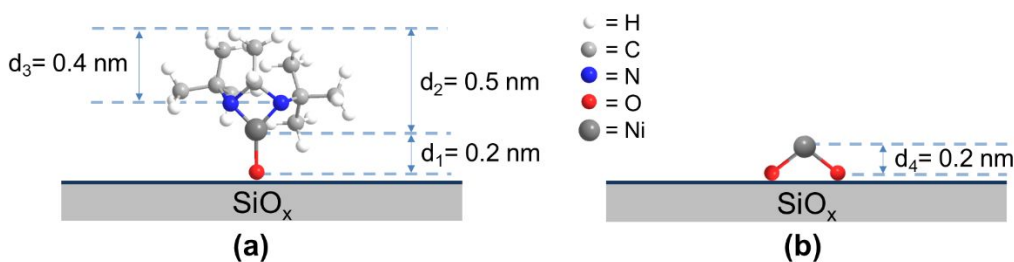| XPS signal				
	Ni 2p	O 1s	N 1s	C 1s
Binding energy (eV)	857	531	400	285
Kinetic energy (eV) (E)	629	955	1086	1201
Bulk Sensitivity factor (S_{bulk})[a]	20.76	2.89	1.68	1.00
Surface Sensitivity factor (S_{surf})	31.81	3.36	1.80	1.00

[a]Bulk sensitivity factors are adopted from Thermo Advantage (v5.945).

According to Wagner's paper on sensitivity factors (*J. Electron Spectrosc. Relat. Phenom.* **1983**, 32, 99−102), the surface sensitivity factors (rather than the conventional bulk sensitivity factors) should be used for the quantitative XPS analysis of the surface atoms. Note that the (bulk) sensitivity factors (S_{bulk}) listed in common database (e.g. Thermo Advantage (v5.945)) are derived for bulk materials, which assumes that the material is of the thickness at least several times the length of the photoelectron mean free path (λ); however, this is not applicable for surface adsorbates because the size of the adsorbates is usually smaller than λ. To this end, a new set of sensitivity factors, namely the surface sensitivity factors (S_{surf}), should be used for the analysis of surface atoms. The set of S_{surf} can be derived from that of S_{bulk}, following $S_{surf} = S_{bulk}/\lambda$, and the photoelectron mean free path (λ) can be reasonably characterized by $\lambda = \alpha E^{0.66}$ (cf. Wagner's paper), where E is the photoelectron kinetic energy. By adopting the normalization to give $S_{surf}(C1s) = 1$, we arrive at $S_{surf} = S_{bulk} (E_{C1s}/E)^{0.66}$, which is used to calculate the S_{surf} data shown in Table S4.
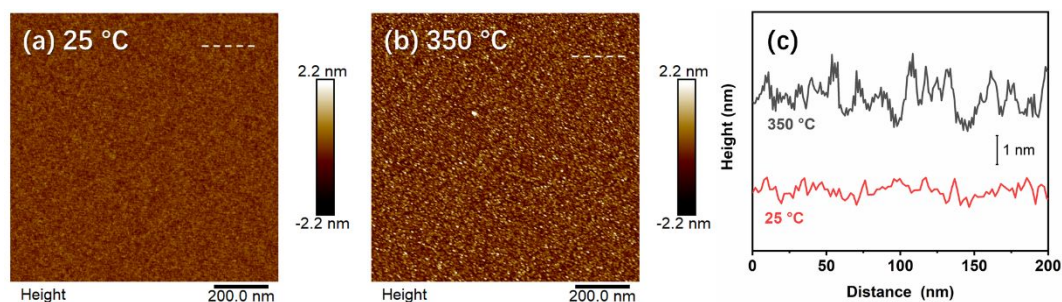
Figure S4. Ex situ atomic force microscopy (AFM, Bruker, Multimode 8) images of (a) a $Ni(amd)_2$-dosed SiO_x/Si sample and (b) a $Ni(amd)_2$-dosed SiO_x/Si sample subjected to the post-dose heat treatment at 350 °C. In both cases, the $Ni(amd)_2$ was dosed at 25 °C. (c) Height profiles along the dashed lines drawn in (a) and (b). While the sample surface remained fairly flat after the $Ni(amd)_2$ dose at 25 °C, the 350 °C heat treatment substantially roughened the surface by creating nanoparticular features on the surface. The height profile (c) suggests that the size of the nanoparticles was about 1 nm. It is worth noting that the lateral size of the nanoparticles was largely exaggerated in the AFM image because of the size of the AFM tip; nevertheless, the height information revealed from the AFM image should be accurate.

Figure S5. Estimation of the XPS signal attenuation by the surface (a) −O−Ni−amd **(I)** and (b) O−Ni−O **(II)** moieties.

(c)

Photoelectron mean free path λ (nm)[a]			
	Ni 2p	O 1s	N 1s
in amidinate layer[b]	2.0 (λ_{Ni})	2.7 (λ_{O2})	3.0 (λ_{N})
in Ni layer	-	1.5 (λ_{O1})	-

[a]Data are adopted from the NIST database (Powell, C. J.; Jablonski, A. NIST Electron Inelastic-Mean-Free-Path Database, version 1.2, SRD 71; National Institute of Standards and Technology: Gaithersburg, MD, 2010).

[b]Data of polystyrene are adopted to approximate the amidinate moiety.

It is well known that for a homogenous capping layer with uniform thickness of d, the measured (attenuated) XPS signal intensity (I_{meas}) can be described by $I_{meas} = I_0 \exp(-d/\lambda)$, where I_0 is the intensity if there is no capping layer and λ is the photoelectron mean free path in the capping layer. (The photoelectron takeoff angle is 90°.) Strictly speaking, I_0 should be used to quantify the surface atoms (such as Figure 5), however, because the "capping" layer is ill-defined in both structures **(I)** and **(II)**, the attenuation effect cannot be treated rigorously. Therefore, we simply used I_{meas} to quantify the surface atoms to obtain Figure 5. In the following, we will estimate the error that may be induced by using I_{meas} for the quantitative analysis.

We still adopt the general idea of the exponential decay [$\exp(-d/\lambda)$] to describe the XPS signal attenuation, although some estimations are needed for d's and λ's. The estimations of d's are depicted in Figure S5a,b, where the d's describe the distances for which the photoelectrons generated on different atoms need to travel before entering into vacuum (for $d_{2\sim4}$) or another later (for d_1). The values of λ's (Figure S5c) are adopted from the NIST database for different photoelectron kinetic energies. Note that we use the data for polystyrene (a representative organic polymer) to approximate the amidinate moiety layer, because the latter does not exist in standard database. The detailed calculations are the following:

For the structure **(I)**:

$I_{meas}(\text{Ni})/I_0(\text{Ni}) = \exp(-d_2/\lambda_{\text{Ni}}) = \exp(-0.5/2.0) = 0.778$

$I_{meas}(\text{O})/I_0(\text{O}) = \exp(-d_2/\lambda_{\text{O2}})\exp(-d_1/\lambda_{\text{O1}}) = \exp(-0.5/2.7)\exp(-0.2/1.5) = 0.727$

$I_{meas}(\text{N})/I_0(\text{N}) = \exp(-d_3/\lambda_{\text{N}}) = \exp(-0.4/3.0) = 0.875$

Normalizing to the Ni intensity gives:

$I_{meas}(\text{O})/I_{meas}(\text{Ni}) = 0.934\ I_0(\text{O})/I_0(\text{Ni})$ [i.e. ~7% underestimation]

$I_{meas}(\text{N})/I_{meas}(\text{Ni}) = 1.125\ I_0(\text{N})/I_0(\text{Ni})$ [i.e. ~12% overestimation]

For the structure **(II)**:

$I_{meas}(\text{Ni})/I_0(\text{Ni}) = 1$

$I_{meas}(\text{O})/I_0(\text{O}) = \exp(-d_4/\lambda_{\text{O1}}) = \exp(-0.2/1.5) = 0.875$

Normalizing to the Ni intensity gives:

$I_{meas}(\text{O})/I_{meas}(\text{Ni}) = 0.875\ I_0(\text{O})/I_0(\text{Ni})$ [i.e. ~12% underestimation]

Given the above calculation, we can conclude that using I_{meas} for the quantitative XPS analysis would only cause slight underestimation of the O content (7~12%) and slight overestimation of the N content (12%). These small errors will not substantially alter the discussion and conclusions in the paper. Therefore, for simplicity with reasonable accuracy but not to make too many assumptions, we simply used I_{meas} for the quantitative XPS analysis to obtain Figure 5.
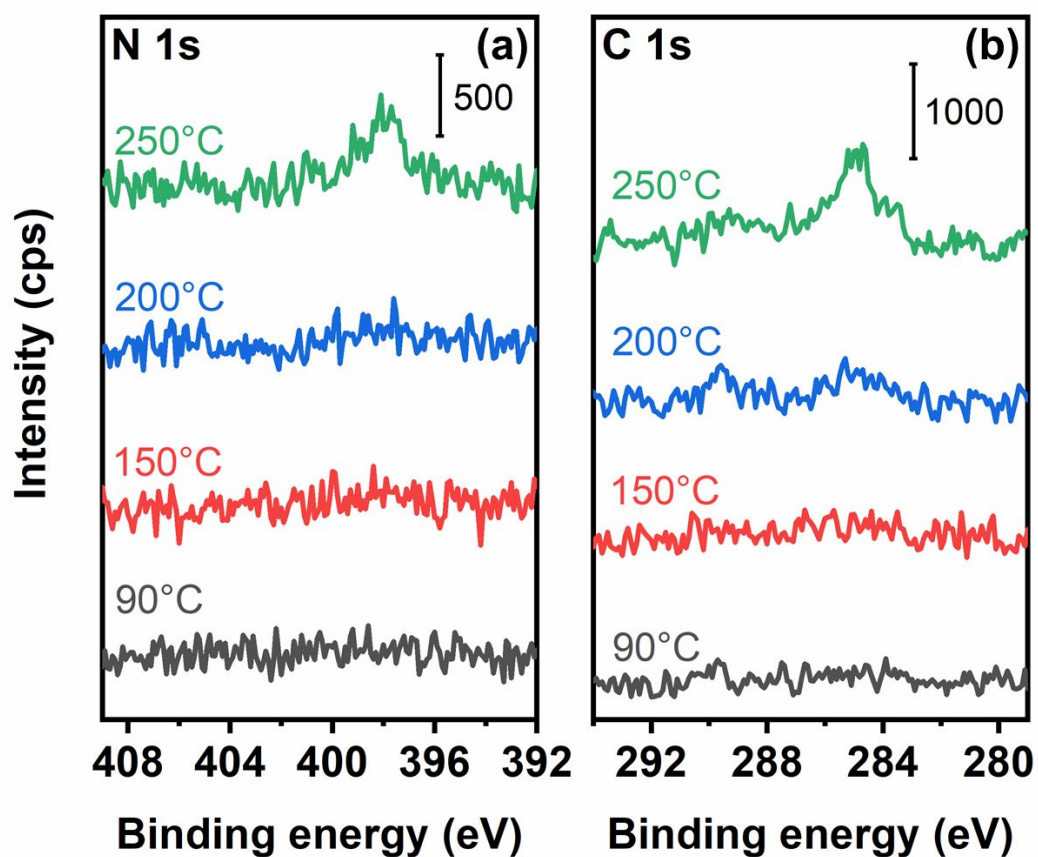
Figure S6. XPS N 1s and C 1s spectra for the ALD NiO films deposited at various temperatures. Drastic increase of the C and N contents can be seen for the temperature at 250 °C.